Available online at www.sciencedirect.com
ScienceDirect
Journal of Power Sources 160 (2006) 1225–1229
JOURNAL OF POWER SOURCES
www.elsevier.com/locate/jpowsour

Short communication

Cobalt plating of high temperature stainless steel interconnects

Xiaohua Deng *, Ping Wei, M. Reza Bateni, Anthony Petric

Department of Materials Science and Engineering, McMaster University, Hamilton, Ont., Canada L8S 4L7

Received 16 December 2005; received in revised form 8 March 2006; accepted 10 March 2006
Available online 27 April 2006

Abstract

To limit oxidation and protect against loss of conductivity in stainless steel for applications such as high temperature fuel cell interconnects, a layer of cobalt was electroplated on the surface. When heated in air at 800 °C, the cobalt was converted into spinel phases containing cobalt, chromium and iron. The oxide layer was characterized by X-ray diffraction and energy dispersive spectrometry. The area specific resistance (ASR) of the samples was measured by a new technique. After 1900 h oxidation at 800 °C in air, the cobalt-coated UNS430 stainless steel had a clean surface and a stable ASR of 0.026 Ω cm^2 compared to uncoated UNS430 which showed a thick, porous oxide growth and an ASR more than 10-fold higher.

Keywords: Solid oxide fuel cells; Interconnect; Ferritic stainless steel; Protective coatings; Cobalt; Spinels

1. Introduction

Interconnects for planar solid oxide fuel cell (SOFC) stacks are almost exclusively made of ferritic stainless steel, e.g., UNS430, Crofer 22 and Hitachi ZMG 232. Ferritic steels offer advantages of low cost, ready availability, high electric and thermal conductivity and thermal expansion match with ceramic cell components. The disadvantage of metal interconnects is the growth of an oxide scale which increases the bulk resistance and contact resistance, and is prone to spalling, particularly on the air electrode side. In addition to deterioration of the electrical contact, the growing scale exacerbates the sealing problem. Furthermore, chromium in the scale forms high temperature volatile species which have been associated with cell poisoning [1]. All of these factors contribute to long-term cell performance degradation.

To solve the problem, different coatings have been proposed and developed. (La, Sr)MnO_3 slurry was dip-coated on Fe–Cr alloys and tested for more than 2600 h with an almost constant, low, area specific resistance (ASR, resistance per unit area) [2]. The oxide coating is sintered at a high temperature, using a reducing atmosphere to limit oxidation of the alloy. However, even when sintered at a high temperature, the oxide layer contains residual porosity. Co–Mn spinel powder [3] was investigated as a protective coating on 430 stainless steel by slurry-spraying and an ASR of approximately 0.5 Ω cm^2 was predicted after 50,000 h operation in air. $LaCrO_3$ thin films [4] and Cr–Al–N coatings [5] have been deposited on stainless steel by radio frequency (rf) magnetron sputtering. Yttria–silver and praseodymia coatings [6] were applied to UNS430 stainless steel by cathodic electrolytic deposition. Manganese [7] and Cu + Fe (converted to $CuFe_2O_4$) [8] were deposited on stainless steel and showed promising protective performance. A manganese-containing ferritic stainless steel, Crofer22 APU, was developed to have oxidation protection and electrical conductivity at higher temperatures [9]. When protective oxide layers of $La_{0.85}Sr_{0.15}MnO_{3-\delta}$ and $Mn_{2-x}Cr_xO_4$ were sputtered on a Ni–Cr alloy, the oxidation rate of the alloy exhibited linear behavior with time, indicating that the coatings were effective in reducing the oxidation kinetics [10].

This research focused on cobalt coating of UNS430 stainless steel using the cost-effective technique of electroplating. After oxidization at typical SOFC operating temperature, the cobalt forms a spinel compound or solution, and maintains high density without the need for high temperature sintering. Cobalt spinels have relatively high electrical conductivities [11] and the chromium oxide that forms from the alloy is either covered by a dense spinel layer or dissolves in the spinel and hence has lower activity.

* Corresponding author. Tel.: +1 905525 9140x24886.
E-mail address: dengx@mcmaster.ca (X. Deng).

0378-7753/$ – see front matter © 2006 Elsevier B.V. All rights reserved.
doi:10.1016/j.jpowsour.2006.03.024

2. Experimental

The electroplating solution was made by dissolving 137 g of $CoSO_4 \cdot 7H_2O$ and 33 g of $CoCl_2 \cdot 6H_2O$ in 500 g of distilled water and 6.2 g of H_3BO_3 was added to the solution [12]. The UNS430 stainless steel substrate was washed in ethanol and distilled water, and used as the cathode; platinum foil was used as the anode. Cobalt metal was electroplated on the surface at a current of 22 mA cm^{-2} for 10–20 min, resulting in a 20–40 μm micron thick coating. The sample was rinsed with distilled water and dried, then heat-treated at 1000 °C for 2 h in forming gas (7% $H_2 + N_2$). The heat treatment was used to bond the metal coating layer to the substrate before oxidation.

Electrical conductivity of the coated steel was measured at 800 °C in air by a new technique. The measurement apparatus (Fig. 1) was designed to evaluate the coating and oxide scale layer only, and avoid interference from other contact resistances. Two rods of UNS430 stainless steel, 1/4 in. diameter (A-1 Wire Tech, Inc.), were plated with cobalt on one end by the procedure described above, followed by heat treatment at 1000 °C in forming gas. Thin layers of porous Pt paste were applied on the cobalt-coated surfaces by a wooden splint. After drying at 200 °C, the two rods of stainless steel were placed end to end in a furnace. The porous layer of platinum (Fig. 2) assured both oxygen access to the coated layers and electronic contact between the coated ends. Another pair of steel rods, without cobalt coating, was used as a control sample. A constant dc current density of 1.5 A cm^{-2} was applied through the rods, while voltage and temperature were measured and recorded by computer. Similar samples were oxidized at 800 °C in air to be characterized by X-ray diffraction (XRD), SEM and energy dispersive spectrometry (EDS).

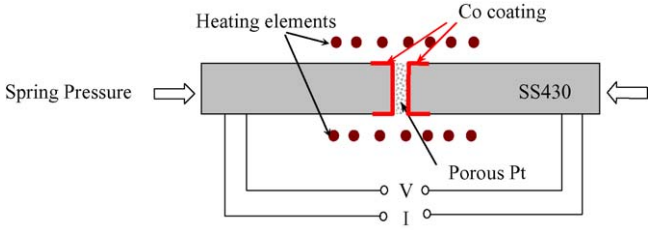

Fig. 1. Schematic diagram of measurement apparatus.

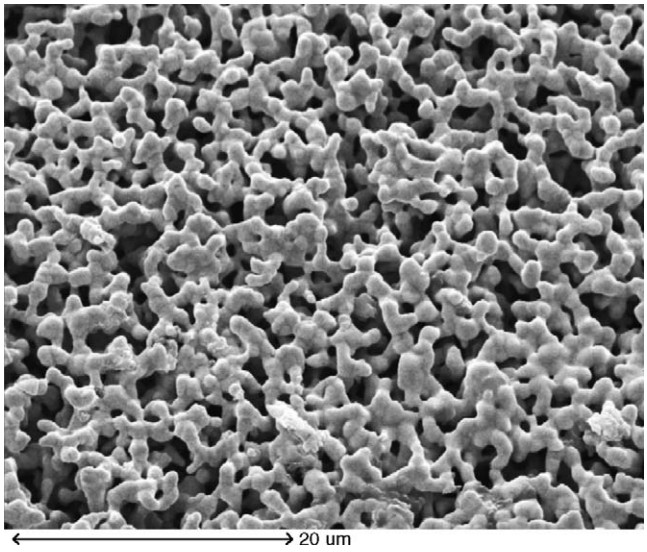

Fig. 2. SEM micrograph of porous platinum layer (sintered at 850 °C for 1 h).

3. Results and discussion

3.1. X-ray diffraction

The cobalt coating was examined by XRD as-deposited, after 1 h oxidation and after 9 days oxidation (Fig. 3). The as-deposited cobalt exhibited a hexagonal structure (Fig. 3a). After 1 h at 800 °C, the cobalt was oxidized to cobalt oxide and mixed spinel phases. The X-ray spectrum in Fig. 3b matches that of Co_2CrO_4 except for a peak near 65° which sits between peaks of Co_3O_4 and Co_2CrO_4 spinel phases. After 220 h oxidation at 800 °C, the Co_3O_4 phase vanished and new spinel phases, $CoCrFeO_4$ and $CoCr_2O_4$, appeared in addition to Co_2CrO_4 (Fig. 3c). Thus, long-term oxidation resulted in mixed spinel phases.

3.2. Electrical conductivity

The area specific resistance of uncoated and cobalt-coated UNS430 was measured (Fig. 1) at 800 °C in air with a constant dc current density of 1.5 A cm^{-2}. Fig. 4 shows the area specific

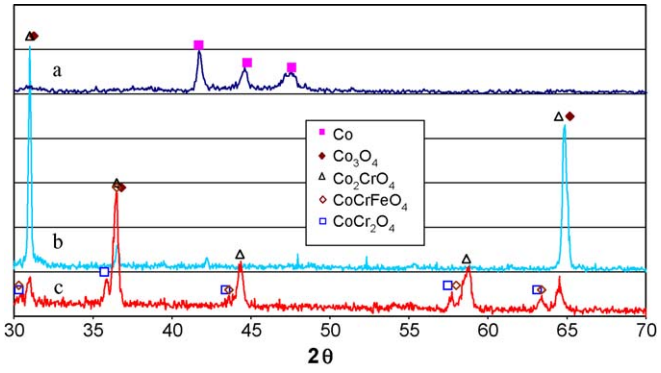

Fig. 3. XRD spectra of cobalt-coated 430 stainless steel: (a) as-deposited, (b) after 1 h oxidation and (c) after 220 h oxidation in air at 800 °C.

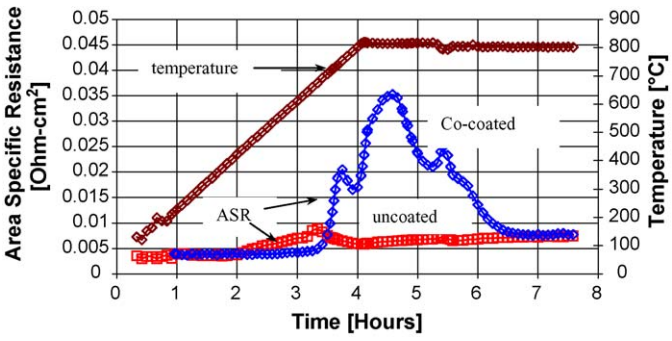

Fig. 4. ASR change with time of uncoated and cobalt-coated UNS430 stainless steel.

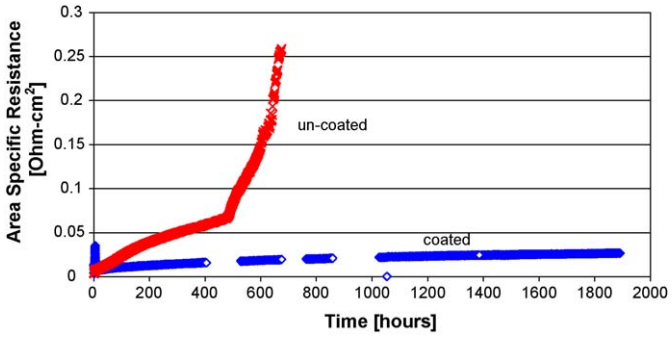

Fig. 5. ASR changes for uncoated and cobalt-coated UNS430 stainless steel at 800 °C in air.

resistance changes during the heating at a rate of 200 °C h^{-1} up to 800 °C. The uncoated steel did not show obvious resistance change during the heating up phase, whereas the ASR of the cobalt-coated sample showed a large ASR peak, beginning at 650 °C and decreasing back to the base level of the uncoated steel after several hours at 800 °C. During that time, the cobalt coating was oxidized and subsequently formed spinel solutions with chromium and iron.

As the oxidation continued, the scale on the uncoated steel showed a parabolic type increase in the ASR until the measurement ran off scale at around 500 h, followed by a runaway type of increase in resistance after that point. The ASR of the cobalt-coated steel increased linearly at a relatively low rate compared with the uncoated sample in good agreement with Armstrong et al. [10]. After oxidation at 800 °C in air for more than 1900 h, the cobalt-coated steel continued to demonstrate good oxidation resistance with an ASR of 0.026 Ω cm^2 (Fig. 5).

3.3. Microstructures and phase analysis

The surface and cross-section of coated samples were examined after heat treatment at 1000 °C in forming gas (7% H_2 + N_2). The SEM photograph of the surface of the cobalt coating (Fig. 6a) shows a grain size of 10–50 μm. With reciprocal diffusion of cobalt, chromium and iron at 1000 °C, a mixed Co–Fe–Cr layer forms at the surface (Fig. 6b) and no boundary is visible between the UNS430 and coating layer. No nitrogen or oxygen was detected in these samples.

Additional uncoated and cobalt-coated UNS430 samples were also oxidized in air at 800 °C. After 220 h oxidization, the uncoated stainless steel grew a black oxide scale which spalled from the surface in some areas, while the cobalt-coated steel exhibited a grey, shiny surface (Fig. 7).

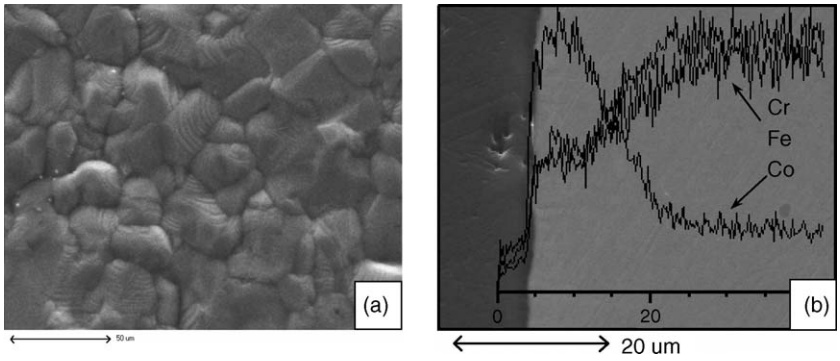

Fig. 6. (a) SEM photo of cobalt plated surface after 2 h at 1000 °C in forming gas. (b) EDS elemental distributions of cobalt, chromium and iron across the UNS430 interface.

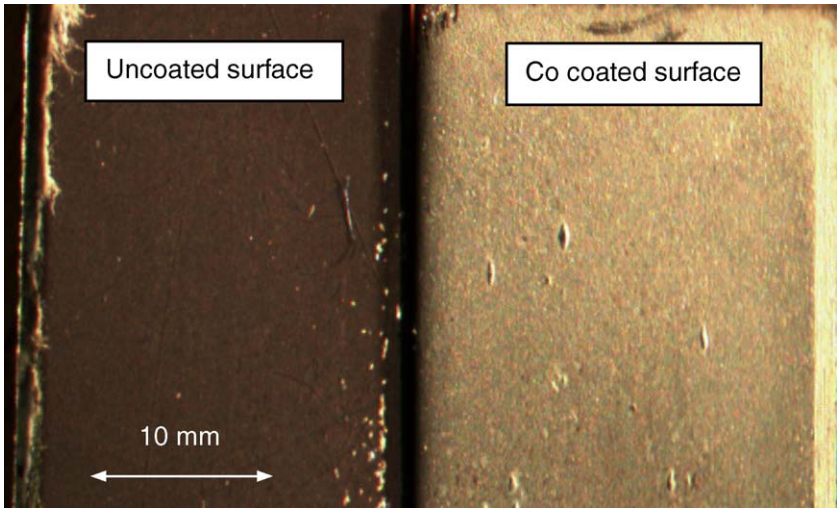

Fig. 7. Uncoated and cobalt-coated UNS430 surface after 220 h oxidation in air at 800 °C.

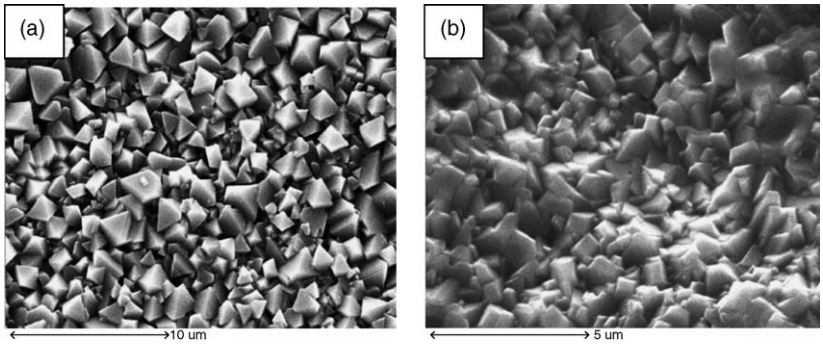

Fig. 8. SEM micrographs of (a) uncoated and (b) cobalt-coated UNS430 surface after 220 h oxidation in air at 800 °C.

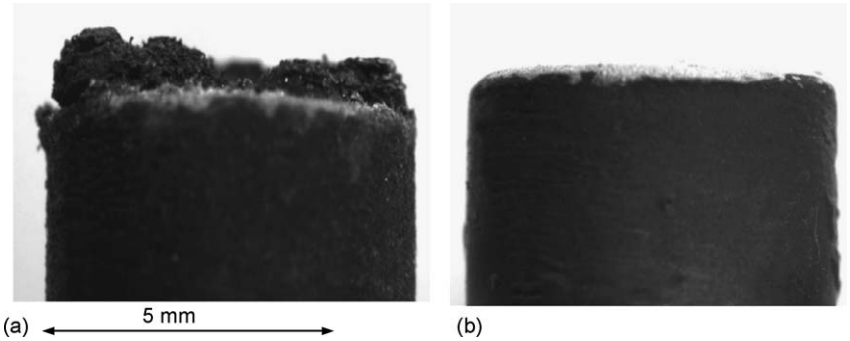

Fig. 9. Photos of scale on ends of (a) uncoated and (b) cobalt-coated UNS430 stainless steel rods after 1900 h oxidation in air at 800 °C.

SEM micrographs of the samples show a porous oxide scale layer with pyramidal grains on the surface of the uncoated sample (Fig. 8a) and the oxide scale detached or spalled from the steel. The oxide scale on the cobalt-coated UNS430 surface exhibited a smaller grain size and much denser packing (Fig. 8b), which is similar to Yang's results [9].

The steel rods from the ASR measurement were examined by optical microscope and SEM after 1900 h oxidation in air at 800 °C. The uncoated sample developed a heavy, friable, porous Fe-rich oxide approaching 1 mm thick (Fig. 9a), whereas the cobalt-coated sample had a clean, smooth surface (Fig. 9b).

The scale on the uncoated sample was partially spalled (Fig. 10a) and it was not possible to mount and polish the full scale layer. Meanwhile, the cobalt-coated steel had a continuous oxide layer covering its surface (Fig. 10b).

Fig. 11 shows an SEM micrograph and elemental mapping of the cross-section of the cobalt-coated sample after 1900 h. The oxide scale layer consists of spinel phases containing cobalt, chromium and iron. Cobalt occupies most of the outer layer but also appears in the steel substrate. A dense chromium oxide layer is concentrated at the interface between the steel and outer oxide. Iron has diffused through the chromium oxide scale, forming an iron-rich band, followed by a gradient through the cobalt oxide. Similar results were observed in the sample oxidized for 220 h.

The combined evidence of imaging, diffraction, conductivity and analysis leads to a hypothesis of how cobalt metal coatings

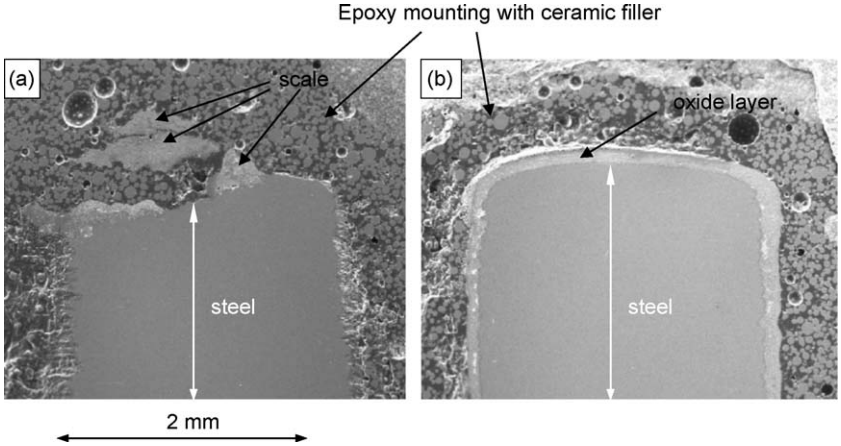

Fig. 10. SEM cross-section micrograph of (a) uncoated and (b) cobalt-coated UNS430 stainless steel rods after 1900 h oxidation in air at 800 °C. Note that the granular material surrounding the sample is the mounting compound with ceramic filler.

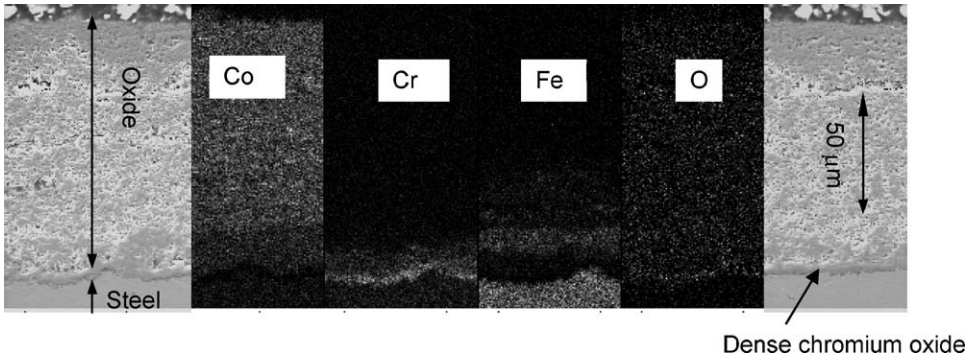

Fig. 11. Micrograph and elemental maps of cross-section of cobalt-coated UNS430 after 1900 h oxidation in air at 800 °C.

enhance the corrosion protection of stainless steels at 800 °C. A comparison of photographs after 220 h (Fig. 7) and 1900 h (Fig. 9) reveals a visible difference in the extent of oxidation between coated and uncoated samples. It shows that alloying with 16% Cr alone is not sufficient to protect steel from oxidation at 800 °C. The addition of an external layer of cobalt is not by itself expected to protect the steel because it is readily oxidized. It must be used in combination with a Cr_2O_3-forming steel. Cobalt is the preferred cladding material because its oxides, CoO and Co_3O_4, as well as $CoCr_2O_4$ have conductivities of 6–7 S cm^{-1} at 800 °C [11], two orders of magnitude higher than Cr_2O_3.

Fig. 11 shows that Cr is restricted to a continuous and dense layer at the metal oxide interface and the absence of Co or Fe in this region implies that this layer is Cr_2O_3. One can see that Fe has diffused across the layer to form an iron-rich bond. The outer scale is dominated by cobalt, although both Fe and Cr are present in small amounts. It is not possible to conclude from data whether this is a homogenous spinel solid solution on a mixed phase solution. However, it is apparent that without the cobalt layer, the Fe–Cr alloy forms a porous oxide with poor mechanical integrity and low conductivity. The cobalt oxide coating plays a key role in limiting the oxidation rate and the evaporation of chromium, thus helping to maintain the integrity of the Cr_2O_3 layer at the interface and a compact, conductive, surface scale.

4. Conclusion

UNS430 stainless steel was electroplated with cobalt as a measure to improve high temperature conductivity and to reduce the chromium evaporation. The cobalt was oxidized to Co_3O_4 which reacted with iron and chromium forming a layer of mixed spinels. The coating not only maintains electrical contact, but it offers oxidation protection in ferritic stainless steels at lower chromium content and it is capable of significantly retarding chromium evaporation which reduces chromium poisoning of fuel cell. Stainless steel UNS430 with the cobalt layer showed a low ASR of 0.026 Ω cm^2 after 1900 h oxidation at 800 °C. Electroplating is a cost-effective way to apply such coatings, but other techniques such as cladding, vapor deposition or ceramic processing methods will achieve the same objectives.

Acknowledgements

The authors wish to acknowledge the financial support of the Natural Sciences and Engineering Research Council of Canada and Fuel Cell Technologies Ltd.

References

[1] S.C. Paulson, V.I. Birss, in: S.C. Singhal, M. Dokiya (Eds.), Proceedings of the International Symposium on Solid Oxide Fuel Cells VIII, The Electrochemical Society, Pennington, NJ, 2003, pp. 498–508.
[2] J.-H. Kim, R.-H. Song, S.-H. Hyun, Solid State Ionics 174 (2004) 185–191.
[3] X. Chen, P.Y. Hou, C.P. Jacobson, S.J. Visco, L. De Jonghe, Solid State Ionics 176 (5–6) (2005) 425–433.
[4] N. Orlovskaya, A. Coratolo, C. Johnson, R. Gemmen, J. Am. Ceram. Soc. 87 (10) (2004) 1981–1987.
[5] P.E. Gannon, et al., Surf. Coat. Technol. 188–189 (2004) 55–61.
[6] P. Wei, I. Zhitomirsky, A. Petric, in: S.C. Singhal, J. Mizusaki (Eds.), Proceedings of Symposium on Solid Oxide Fuel Cells IX, vol. 2005–07, The Electrochemical Society, Pennington, NJ, 2005, pp. 1851–1858.
[7] T.J. Armstrong, M.A. Homel, A.V. Virkar, in: S.C. Singhal, M. Dokiya (Eds.), Proceedings of Symposium on Solid Oxide Fuel Cells VIII, The Electrochemical Society, Pennington, NJ, 2003, pp. 841–850.
[8] R.N. Basu, N. Knott, A. Petric, in: S.C. Singhal, J. Mizusaki (Eds.), Proceedings of Symposium on Solid Oxide Fuel Cells IX, The Electrochemical Society, Pennington, NJ, 2005, pp. 1859–1865.
[9] Z. Yang, J.S. Hardy, M.S. Walker, G. Xia, S.P. Simner, J.W. Stevenson, J. Electrochem. Soc. 151 (11) (2004) A1825–A1831.
[10] T.J. Armstrong, M. Smith, A.V. Virkar, in: S.C. Singhal, J. Mizusaki (Eds.), Proceedings of Symposium on Solid Oxide Fuel Cells IX, The Electrochemical Society, Pennington, NJ, 2005, pp. 1795–1805.
[11] H. Ling, A. Petric, in: S.C. Singhal, J. Mizusaki (Eds.), Proceedings of Symposium on Solid Oxide Fuel Cells IX, vol. 2005–07, The Electrochemical Society, Pennington, NJ, 2005, pp. 1866–1873.
[12] H. Ling, High temperature electrical and thermal properties of transition metal spinel oxides, MASc. Thesis, McMaster University, 2004.